Generating iPSC-Derived Choroidal Endothelial Cells to Study Age-Related Macular Degeneration

Allison E. Songstad,[1] Luke A. Wiley,[1] Khahn Duong,[2] Emily Kaalberg,[1] Miles J. Flamme-Wiese,[1] Cathryn M. Cranston,[1] Megan J. Riker,[1] Dana Levasseur,[2] Edwin M. Stone,[1,3] Robert F. Mullins,[1] and Budd A. Tucker[1]

[1]Stephen A. Wynn Institute for Vision Research, Department of Ophthalmology and Visual Sciences, University of Iowa, Iowa City, Iowa, United States
[2]Department of Internal Medicine, University of Iowa, Iowa City, Iowa, United States
[3]Howard Hughes Medical Institute, University of Iowa, Iowa City, Iowa, United States

Correspondence: Budd A. Tucker, Stephen A. Wynn Institute for Vision Research, University of Iowa, 375 Newton Road, MERF 4156, Iowa City, IA 52246, USA; budd-tucker@uiowa.edu.

Submitted: April 10, 2015
Accepted: November 3, 2015

Citation: Songstad AE, Wiley LA, Duong K, et al. Generating iPSC-derived choroidal endothelial cells to study age-related macular degeneration. *Invest Ophthalmol Vis Sci*. 2015;56:8258–8267. DOI:10.1167/iovs.15-17073

Purpose. Age-related macular degeneration (AMD), the most common cause of incurable blindness in the western world, is characterized by the dysfunction and eventual death of choroidal endothelial (CECs), RPE, and photoreceptor cells. Stem cell–based treatment strategies designed to replace photoreceptor and RPE cells currently are a major scientific focus. However, the success of these approaches likely also will require replacement of the underlying, supportive choroidal vasculature. The purpose of this study was to generate stem cell–derived CECs to develop efficient differentiation and transplantation protocols.

Methods. Dermal fibroblasts from the *Tie2-GFP* mouse were isolated and reprogrammed into two independent induced pluripotent stem cell (iPSC) lines via viral transduction of the transcription factors *Oct4*, *Sox2*, *Klf4*, and *c-Myc*. *Tie2-GFP* iPSCs were differentiated into CECs using a coculture method with either the RF6A CEC line or primary mouse CECs. Induced pluripotent stem cell–derived CECs were characterized via RT-PCR and immunocytochemistry for EC- and CEC-specific markers.

Results. Induced pluripotent stem cells generated from mice expressing green fluorescent protein (GFP) under control of the endothelial *Tie2* promoter display classic pluripotency markers and stem cell morphology. Induced pluripotent stem cell–derived CECs express carbonic anhydrase IV, eNOS, FOXA2, PLVAP, CD31, CD34, ICAM-1, Tie2, TTR, VE-cadherin, and vWF.

Conclusions. Induced pluripotent stem cell–derived CECs will be a valuable tool for modeling of choriocapillaris-specific insults in AMD and for use in future choroidal endothelial cell replacement approaches.

Keywords: induced pluripotent stem cells, choroidal endothelial cells, macular degeneration

Age-related macular degeneration (AMD) is the leading cause of irreversible blindness in the developed world.[1] Aging is the most important risk factor for developing AMD. One study collected data from the United States, Europe, and Australia to show that the prevalence of AMD increased from 0.2% in people between 55 and 64 years old to more than 13% in people 85 years and older.[2] As the successes of modern medicine continue to increase the average human life span, that is, the population of individuals above the age of 75 in the United States is predicted to rise by 48% between 2010 and 2025, the negative societal impact of AMD is expected to worsen.[3,4] In the United States alone, approximately two million people suffer from severe, end-stage AMD and are legally blind.[1,2] An additional seven million individuals are afflicted with early-stage AMD, predisposing them to suffer advanced AMD involving the loss of choroidal vasculature, RPE, and photoreceptor cells.[3]

Age-related macular degeneration is characterized by early and intermediate stages that exhibit morphological alterations in the retina and underlying choroid. Its most salient feature is the presence of drusen deposits between the RPE and choriocapillaris, which may disrupt the transport of oxygen and nutrients leading to dysfunction and death of the RPE and, eventually photoreceptor cells.[5–9] Early/intermediate AMD can progressively worsen, leading to advanced AMD (geographic atrophy and/or choroidal neovascularization, both of which result in severe vision loss). Therapies that target VEGF, such as bevacizumab and ranibizumab, have proven efficacious in treatment of neovascular (wet) AMD. However, the only treatment presently offered for atrophic (dry) AMD, the most common subgroup, is dietary vitamin supplementation, which offers incomplete benefits in slowing progression.[10] Deciphering the pathophysiological mechanisms of dry AMD will be important for development of early intervention strategies.

Age-related macular degeneration impacts three interdependent cell types located within the outer retinal unit, namely the light-sensing photoreceptor cells, underlying RPE, and choroidal endothelial cells (CECs) that comprise the distinctive vasculature of the choriocapillaris. Loss of any one of these three cell types can have a negative impact on the homeostasis and integrity of the other two. Historically, the RPE has long been considered to be the key cell type in AMD pathogene-

Table 1. Primers Used to Amplify Coding Sequences

EGFP P2A fusion-F1	CACCGTCGACCACCATGGTGAGCAAGGGCGAGGA
EGFP P2A fusion-R1	GGATCCCTTGTACAGCTCGTCCATGCC
mKOrange2 P2A fusion-F1	CACCGTCGACCACCATGGTGAGCGTGATCAAGCCC
mKOrange2 P2A fusion-R1	GGATCCGGAGTGGGCCACGGCGTC
mTagBFP P2A fusion-F1	CACCGTCGACCACCATGAGCGAGCTGATTAAG
mTagBFP P2A fusion-R2	GGATCCATTAAGCTTGTGCCC
GSG sequence	GGATCCGGCGCCACCAACTTCAGCCTGCTGAAGCAGGCCGGCGACGTGGAGGAGAACCCCGGCCCC
mOct4 P2A fusion-F	GCTCTGGATCCGGCGCCACCAACTTCAGCCTGCTGAAGCAGGCCGGCGACGTGGAGGAGAACCCCGGCCCCATGGCTGGACACCTGGCTT
mOct4 P2A fusion-R	GCTCTGCACTAGTTCAGTTTGAATGCATGGGAGAGCC
mSox2 P2A fusion-F	GCTCTGGATCCGGCGCCACCAACTTCAGCCTGCTGAAGCAGGCCGGCGACGTGGAGGAGAACCCCGGCCCCAT GTATAACATGATGGAGA
mSox2 P2A fusion-R	GCTCTGCACTAGTTCACATGTGCGACAGGGGCA
mc-Myc P2A fusion-F	GCTCTGGATCCGGCGCCACCAACTTCAGCCTGCTGAAGCAGGCCGGCGACGTGGAGGAGAACCCCGGCCCCCTGGATTTCCTTTGGGCG
mc-Myc P2A fusion-R	GCTCTGCACTAGTTTATGCACCAGAGTTTCGAAG
mKLF4 P2A fusion-F	GCTCTGGATCCGGCGCCACCAACTTCAGCCTGCTGAAGCAGGCCGGCGACGTGGAGGAGAACCCCGGCCCCATGGCTGTCAGCGACGCTC
mKLF4 P2A fusion-R	GCTCTGCACTAGTTTAAAAGTGCCTCTTCATGTGTAAGG

sis.[10,11] Although modifications in the RPE are indisputably essential in AMD pathology, recent reports suggest that choroidal alterations, especially dropout of choriocapillaris endothelial cells, occur very early at the onset of disease,[5,6] possibly due to complement activation in the choroid.[9]

We described the use of the *Tie2-GFP* mouse model, which expresses green fluorescent protein (GFP) under the control of the endothelial cell–specific angiopoietin receptor *Tie2* promoter, to generate two independent induced pluripotent stem cell (iPSC) lines.[12] Using these cell lines, we have developed successfully an efficient differentiation protocol capable of generating CEC-like cells that can be used for future disease modeling and cell replacement studies.

Materials and Methods

Ethics Statement

All experiments were conducted with the approval of the University of Iowa Animal Care and Use Committee and were consistent with the Association for Research in Vision and Ophthalmology Statement for the Use of Animals in Ophthalmic and Vision Research and the Declaration of Helsinki.

Generation of OSMK Fluorescence Protein Tagged Plasmids

The coding sequences for murine *Oct4*, *Sox2*, *c-Myc*, and *Klf4*, as well as the fluorescent reporter genes *eGFP*, *mKOrange2*, *mTagBFP*, and *mKate* (Table 1) were PCR amplified using Agilent Pfu Ultra II polymerase (Cat. No. 600850; Agilent Technologies, Santa Clara, CA, USA) and subsequently cloned into the pCR blunt II TOPO vector (Cat. No. K2800; Life Technologies, Grand Island, NY, USA), and confirmed via Sanger sequencing analysis. The primers for *Oct4*, *Sox2*, *c-Myc*, and *Klf4* were engineered with a 5′ Gly-Ser-Gly-P2A linker. Final constructs were built via either two- or three-way ligations, including the coding sequence of each gene of interest and a color tag into a Gateway adapted entry vector. Each fluorescent protein was fused to each gene via a P2A sequence such that *eGFP* was linked to *Oct4*, *mKOrange2* to *Sox2*, *mTagBFP* to *Klf4*, and *mKate* to *c-Myc*, respectively. The lentiviral vector[13] was converted into a Gateway destination vector. Each entry vector was recombined with the lentiviral destination vector via a BP-LR clonase II (Cat. Nos. 11789-020 and 11791-01; Life Technologies) reaction to generate the final lentiviral expression vectors. Concentrated lentiviral supernatant was produced and titered as described previously.[14]

Isolating Primary Choroidal Endothelial Cells

One-week-old mice were euthanized and their eyes were harvested to isolate the choroids. For each eye, the retina was peeled off from the RPE, and the choroid was isolated from the posterior pole and cut into smaller explants using forceps and microdissecting scissors. The choroidal explants were plated on six-well plates in a matrigel matrix. The plated explants were incubated at 37°C for 20 minutes to allow the matrigel to gelatinize. After the matrix formed, the choroidal explants were fed biopsy media (MEMα medium [Cat. No. 12571-063; Gibco Laboratories, Gaithersburg, MD, USA], 10% FBS [Cat. No. 26140-079; Gibco Laboratories], 1% primocin [Cat. No. ant-pm-2; Invivogen, San Diego, CA, USA], 10 ng/mL VEGF [Cat. No. 298-VS-005; R&D Systems, Minneapolis, MN, USA]) with recombinant human VEGF (10 ng/μL). Choroidal endothelial cells migrated out of the matrix and were characterized for expression of various EC and CEC markers via RT-PCR analysis, and were characterized for carbonic anhydrase IV expression using immunolabeling (see below). The primary CECs from the original explants were used for the coculture differentiation protocol described below.

Isolating Tie2-GFP Mouse Fibroblasts

One-month-old *Tie2-GFP* (*Rag1*^{tm1Mom}Tg[*Tie2-GFP*]287Sato/J) mice were used as fibroblast donors. Tail-tip samples were minced and dissociated via incubation in a mixture of 0.25% trypsin (Cat. No. 25200056; Invitrogen, San Diego, CA, USA) and 4 mg/mL collagenase (Cat. No. 07909; Stem Cell Technologies, Vancouver, BC, Canada) at 37°C for 1 hour with constant agitation. Following incubation, tissue was triterated using a polished pasteur pipette and passed through a 40-μm microfilter (Cat. No. 352340; Corning, Inc., Corning, NY, USA) to remove large undigested debris. Liberated cells were plated on collagen- (Cat. No. 354236; Corning, Inc.), laminin- (Cat. No. 23017015; Invitrogen), and fibronectin-coated (Cat. No. AK8350-0005; Akron BioTech, Boca Raton, FL, USA) six-well

tissue culture plates (Cat. No. 3516; Corning), and grown to confluency.

Viral Transduction of Reprogramming Factors

Upon reaching 100% confluency, *Tie2-GFP* fibroblasts were passaged into six-well tissue culture plates at a density of 1.0×10^5 cells/well. Fibroblasts were transduced the following day with either: (1) four separate lentiviral vectors (*mKOrange2*-P2A-*Sox2*, *mEGFP*-P2A-*Oct4*, *mTagBFP*-P2A-*Klf4*, *mKate*-P2A-*c-Myc*) at a multiplicity of infection (MOI) of 3 per vector or (2) with a polycistronic lentiviral vector containing *Oct4*, *Klf4*, *Sox2*, and *c-Myc* (OKSM; Cat. No. SCR510; Millipore, Darmstadt, Germany) at an MOI of 20 with 0.05% polybrene (Cat. No. H9268-5G; Sigma-Aldrich Corp., St. Louis, MO, USA). At 12 to 16 hours after infection with either approach, fibroblasts were washed and fed with fresh pluripotency medium (Dulbecco's modified Eagle's medium [DMEM], F-12 medium [Cat. No. 11320-033; Gibco, Laboratories], 15% FBS [Cat. No. 26140-079; Gibco Laboratories], 0.0008% BME [Cat. No. M6250; Sigma-Aldrich Corp.], 1% 100× nonessential amino acids [NEAA; Cat. No. 11140-050; Gibco Laboratories], and 1.0×10^6 units/L of leukemia inhibitory factor [LIF; mouse; Cat. No. ESG1107; EMD Millipore, Billerica, MA, USA], and 1% primocin [Cat. No. ant-pm-2; Invivogen]). At 5 days after infection, cells were passaged onto 10-cm tissue culture dishes previously coated with irradiated mouse embryonic fibroblasts (IRR-MEF; Cat. No. SCRC-1040.1; ATCC, Manassas, VA, USA) at a density of 1.0×10^5 cells/dish. The cells were fed daily with pluripotency medium. At 3 weeks post-viral transduction, iPSC colonies were isolated and clonally expanded on fresh IRR-MEFs plated on 150 × 25-mm tissue culture dishes (Cat. No. 08-772-24; Corning) for further experimentation. During reprogramming and maintenance of pluripotency, cells were cultured at 5% CO_2 and 37°C.

FACS Analysis of Reprogrammed iPSCs

For iPSC lines generated using four separate fluorescently tagged lentiviral vectors, fully reprogrammed cells that no longer expressed the four transgenes were isolated using the Becton Dickinson Aria II at the University of Iowa Flow Cytometry Core. The collected populations of iPSCs were reseeded on IRR-MEFs and clonally expanded for additional studies.

Reverse Transcription PCR (RT-PCR)

C57BL/6 mouse primary aortic (Cat. No. C57-6052), kidney glomerular (C57-6014G), and brain microvascular (Cat. No. C57-6023) ECs were obtained from Cell Biologics, Inc. (Chicago, IL, USA) and cultured according to the manufacturer's instructions. Total RNA was extracted from cells using the RNeasy Mini-kit (Cat. No. 74104; Qiagen, Valencia, CA, USA) following the manufacturer's protocol. A 100 ng amount of RNA was reverse transcribed and amplified with SuperScriptIII One-Step RT-PCR System with Platinum *Taq* DNA Polymerase (Cat. No. 12574-026; Invitrogen) according to the manufacturer's instructions and 20 pmol of each gene-specific primer set (Table 2). All cycling profiles incorporated a cDNA synthesis cycle at 55°C for 20 minutes, an initial denaturation temperature of 94°C for 2 minutes through 40 amplification cycles (15 seconds at 94°C, 30 seconds at the annealing temperature of each primer, and 1 minute at 68°C) and a final extension at 68°C for 5 minutes. Polymerase chain reaction products were separated by electrophoresis on 2% agarose gels (Cat. No. G800802; Invitrogen).

Teratoma Formation to Assess Pluripotency

Teratomas were induced by intramuscular injection of 4.0×10^6 cells per mouse (two mice total). Teratomas were resected 6 weeks after injection, fixed in 4% paraformaldehyde (Cat. No. 43368; Alfa Aesar, Ward Hill, MA, USA) for 24 hours, dehydrated, and embedded in paraffin wax (Cat. No. 220056-498; VWR, Radnor, PA, USA). Samples were sectioned on a microtome (Model 820; American Optical Company, Buffalo, NY, USA) and a regressive hematoxylin and eosin staining was performed on 10-μm thick sections following deparaffinization and rehydration using an automated slide stainer (Model DRS-601; Sakura Finetech USA Inc., Torrance, CA, USA) in the Central Microscopy Core at the University of Iowa.

Embryoid Body (EB) Formation

Tie2-GFP iPSCs were collected using collagenase treatment (1 mg/mL), washed with pluripotency media, dissociated into single cells via pipetting, and placed into ultralow adhesion plates with EB forming medium (DMEM F-12 medium [Gibco Laboratories], 15% FBS [Cat. No. 26140-079; Gibco Laboratories], 0.0008% β-mercaptoethanol [Sigma-Aldrich Corp.], 1% 100X nonessential amino acids [NEAA; Gibco Laboratories], 1% primocin [Cat. No. ant-pm-2; Invivogen]) for 5 days. Embryoid bodies were isolated and used for CEC differentiation.

Spontaneous Differentiation of iPSCs

Tie2-GFP Line 2 EBs were plated at a density of approximately 30 EBs/well in six-well tissue culture plates coated with collagen (Cat. No. 354236 Corning Life Sciences, Corning, NY, USA), laminin (Cat. No. 23017015; Invitrogen), and fibronectin (Cat. No. AK8350-0005; Akron BioTech). Cells were fed every other day with fresh EC basal media (MEMα medium [Cat. No. 12571-063; Gibco Laboratories], 10% FBS [Cat. No. 26140-079; Gibco Laboratories], 1% primocin [Cat. No. ant-pm-2; Invivogen], 10 ng/mL VEGF [Cat. No. 298-VS-005]; R&D Systems). Cultures were allowed to mature for 30 days beyond the initial appearance of *Tie2-GFP*-positive endothelial cells to ensure adequate time for development of choroidal endothelial cell marker expression.

iPSC Differentiation With Primary Kidney ECs

Tie2-GFP Line 2 EBs were plated at a density of approximately 30 EBs/well in six-well tissue culture plates coated with collagen (Cat. No. 354236; Corning), laminin (Cat. No. 23017015; Invitrogen), and fibronectin (Cat. No. AK8350-0005; Akron BioTech). The following day, 1.0×10^5 primary mouse kidney glomerular ECs (C57-6014G; Cell Biologics, Inc.) were plated directly above the EBs in Transwell Permeable Support 0.4 μm Polycarbonate Membrane 24-mm 6-well inserts (Cat. No. 3412; Corning Life Sciences). Cells were fed every other day with fresh EC basal media (MEMα medium [Cat. No. 12571-063; Gibco Laboratories], 10% FBS [Cat. No. 26140-079; Gibco Laboratories], 1% primocin [Cat. No. ant-pm-2; Invivogen], 10 ng/mL VEGF [Cat. No. 298-VS-005]; R&D Systsems). Cultures were allowed to mature for 30 days beyond the initial appearance of *Tie2-GFP* positive endothelial cells to ensure adequate time for development of choroidal endothelial cell marker expression.

iPSC Differentiation Into CECs Via Coculture With Primary CECs

Tie2-GFP EBs were plated at a density of approximately 30 EBs/well in six-well tissue culture plates coated with collagen (Cat.

Table 2. Primer Sequences

Primer	Forward	Reverse
Carbonic anhydrase	GCAACAGTGGCCAATTAAGAAC	ACCTTGTCTCCTACCTCAATCA
DNMT-1	ATGTCCCTGCCTTCCATAAC	CCAGTTCCAGGAGATCCAATAC
CD31	CACGATTGAGTACGAGGTGAAG	TTCAAACTTGGGAGTGGAGAAG
CD34	AGGGTATCTGCCTGGAACTA	AGAGGTGACCAATGCAATAAGA
ICAM-1	GATGCTCAGGTATCCATCCATC	CACTCTCCGGAAACGAATACA
Lin28	GTGTGAGAGAGAGAGTGTGTATG	CAGGAGGAACAGGTAAGGATAAG
Nanog	ATGCCTGCAGTTTTTCATCC	GAGCTTTTGTTTGGGACTGG
PLVAP	ACCCGTGAGAATGCAGAAC	TGTCCAGCGCGCTAATG
SSEA-1	CCTGTCACCCATGTGAAGAA	CCACAGACAGACTCCACTAAAG
TIE2	GACCAGAAGGATGCAAGTCTTA	TGGCTTCACTAGGGTCATTTC
VE-Cadherin	CCGAGAGAAACAGGCTGAATAC	GGACTTCGTGGGTTTGATGATA
VWF	AAAGCATCTCCATGCCCTAG	TTTACACCGCTGTTCCTCAC
eNOS	CCTCACCGCTACAACATACTT	GGGACACCACATCATACTCATC
FOXA2	AACCTCCCTACTCGTACATCTC	GGGTGGTTGAAGGCGTAAT

No. 354236; Corning), laminin (Cat. No. 23017015; Invitrogen), and fibronectin (Cat. No. AK8350-0005; Akron BioTech). The following day, 1.0 × x10^5 RF/6A primate ECs (Cat. No. CRL-1780; ATCC) or 1.0 × 10^5 primary C57BL/6J CECs were plated directly above the *Tie2-GFP* EBs in Transwell Permeable Support 0.4 μm Polycarbonate Membrane 24-mm 6-well inserts (Cat. No. 3412; Corning). Cells were fed with fresh EC media (MEMα medium [Cat. No. 12571-063; Gibco Laboratories], 10% FBS [Cat. No. 26140-079; Gibco Laboratories], 1% primocin [Cat. No. ant-pm-2; Invivogen], 10 ng/mL VEGF [Cat. No. 298-VS-005]; R&D Systems) every other day to allow developing *Tie2-GFP* iPSC-derived ECs to migrate out of the EB and continue to differentiate.

Immunocytochemistry

Cells were fixed in a 4% paraformaldehyde (Cat. No. 43368; Alfa Aesar) solution and incubated overnight at 4°C in immunoblock buffer (1 × PBS containing 5% normal goat serum [Cat. No. 5425S; Cell Signaling, Danvers, MA, USA], 3% BSA [Cat. No. A30075-100.0; Research Products International Corporation, Mt. Prospect, IL, USA], 0.5% Triton X-100 [Cat. No. T8532; Sigma-Aldrich Corp.], 0.03% sodium azide [Cat. No. 438456; Sigma-Aldrich Corp.]) with antibodies targeted against GFP (Cat. No. ab290; Abcam, Cambridge, MA), CA4 (Cat. No. AF2414; R&D Systems), FOXA2 (Cat. No. 8186P; Cell Signaling Technologies), TTR (Cat. No. 200-901-FM9; Rockland, Limerick, PA, USA), VE-Cadherin (Cat. No. 550548; BD Pharmingen, San Jose, CA, USA), ZO-1 (Cat. No. MABT11; EMD Millipore, Billerica, MA, USA). Subsequently, Cy2-anti-rabbit (Cat. No. 111-225-144; Jackson ImmunoResearch, West Grove, PA, USA), Cy3-anti-mouse (Cat. No. 115-165-146; Jackson ImmunoResearch), or Alexa Fluor 647 goat anti-rat (Cat. No. A21247; Life Technologies, Grand Island, NY, USA) fluorescently conjugated secondary antibodies were used and the samples were analyzed using epifluorescence (EVOS FL; AMG Life Technology) and confocal microscopy (Leica DM 2500 TCS SPE; Leica Microsystems, Wetzlar, Germany). Pseudocoloring was performed using Fiji.[15]

Vector VIP Peroxidase Substrate Staining of Cryopreserved Mouse Choroids

Mouse eyes were fixed in 4% paraformaldehyde (PFA) overnight and the anterior chamber was removed using microscissors. The eyecups were treated with a sucrose gradient: 5 minutes in 5% sucrose three times with a 1 × PBS wash between each incubation, 30 minutes in a solution of 2:1 of 5%:20% sucrose, 1 × PBS wash, 30 minutes in a solution of 1:1 of 5%:20% sucrose, 1 × PBS wash, 30 minutes in a solution of 1:2 of 5%:20% sucrose, 1 × PBS wash, overnight incubation in 20% sucrose at 4°C, and embedded in a 2:1 solution of 20% sucrose:OCT). The sections were treated with Vector VIP Peroxidase Substrate (Cat. No. SK-4600; Vector Laboratories, Burlingame, CA, USA) reagents according to the manufacturer's instructions.

Tali Cytometric Analysis

Induced pluripotent stem cells-CECs were collected using TrypLE (Cat. No. 12604013; Life Technologies), washed once with 1 × PBS, and fixed in 4% PFA for 10 minutes. After fixation, the cells were washed twice, suspended in immunoblock buffer with primary α-GFP antibody, and incubated at 4°C for 1 hour. After incubation, the cells were washed and stained with secondary Cy3-conjugated antibody in immunoblock buffer at 4°C for 30 minutes. Stained cells were loaded into a Tali Cellular Analysis Slide and Cy3-labeled cells were detected. Tali results for each iPSC line were collected in triplicate from three independent experiments.

Culture of Extraocular Endothelial Cells

C57BL/6 mouse primary kidney glomerular endothelial cells (Cat. No. C57-6014G; Cell Biologics, Inc.) were expanded. Heart and lung tissue were harvested from 3-week-old *Tie2-GFP* mice. The tissue was minced and dissociated via incubation in a mixture of 0.25% trypsin (Cat. No. 25200056; Invitrogen) and 4 mg/mL collagenase (Cat. No. 07909; Stem Cell Technologies) at 37°C for 1 hour with constant agitation. Following incubation, tissue was triterated using a polished pasteur pipette and passed through a 40-μm microfilter (Cat. No. 352340; Corning) to remove large undigested debris. Liberated cells were plated on Matrigel-coated (Cat. No. 354234; BD Biosciences, San Jose, CA, USA) 6-well tissue culture plates (Cat. No. 3516; Corning), and grown to confluency. Kidney glomerular and heart/lung endothelial cells were fed with fresh EC media (MEMα medium [Cat. No. 12571-063; Gibco Laboratories], 10% FBS [Cat. No. 26140-079; Gibco Laboratories], 1% primocin [Cat. No. ant-pm-2; Invivogen], 10 ng/mL VEGF [Cat. No. 298-VS-005; R&D Systsems]) every other day.

Karyotyping iPSC Lines

Induced pluripotent stem cell lines 1 and 2 were submitted to the Shivanand R. Patil Cytogenetics and Molecular Laboratory

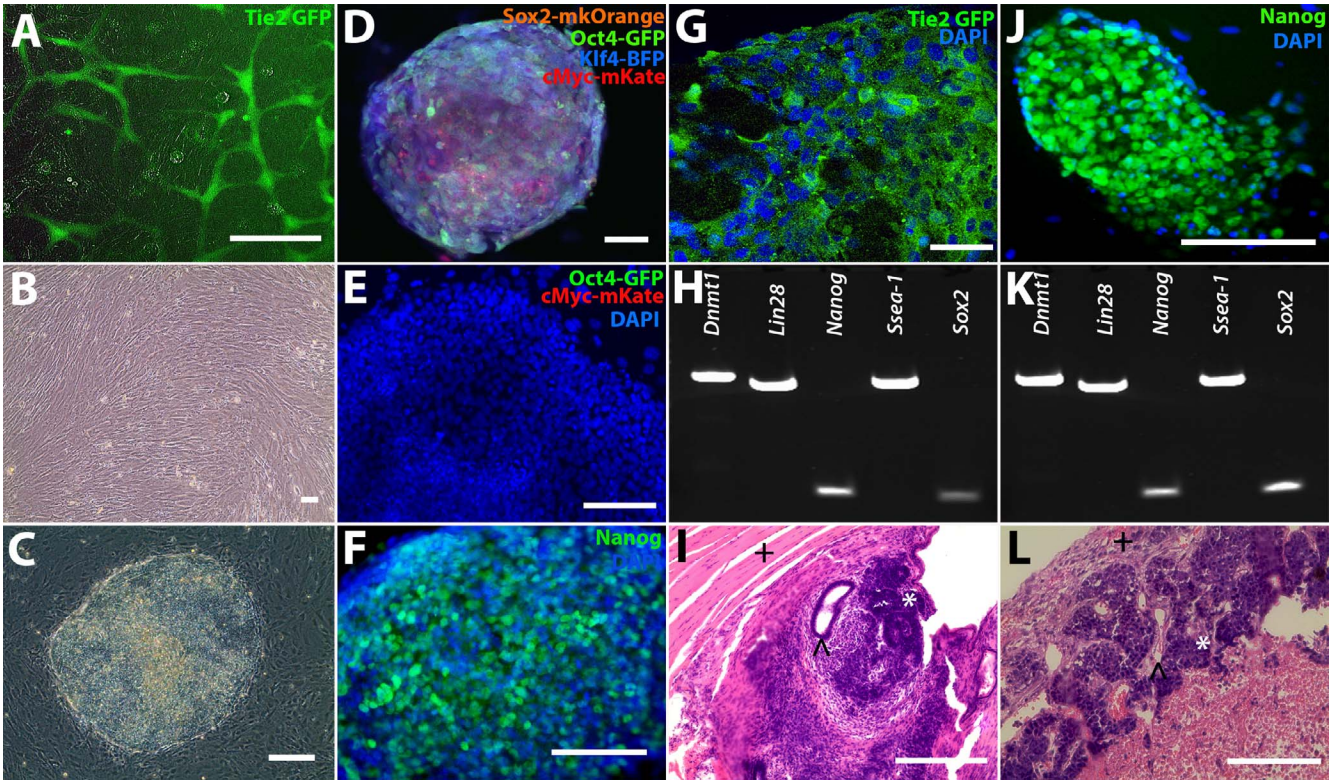

Figure 1. Reprogramming *Tie2* GFP fibroblasts into iPSCs. (**A**) Green fluorescence protein expression in *Tie2-GFP* heart and lung primary ECs. (**B**) Tail-tip fibroblasts were isolated from *Tie2-GFP* mice and reprogrammed into (**C**) iPSCs via transduction with either (**D**) fluorescently tagged lentiviral vectors (iPSC-L1) or a (**J**) polycistronic lentiviral vector (iPSC-L2). (**E**) The FACS iPSC-L1 cells did not express the exogenous fluorescent tags e*GFP-Oct4* and *mKate-c-Myc* (4′,6-diamidino-2-phenylendole [DAPI] = *blue*), but did express (**F**) Nanog, indicating the iPSC-L1 cells were fully reprogrammed. (**G**) iPSC-L1 EBs expressed GFP (*green*), indicating the presence of ECs (DAPI = *blue*). (**H**, **K**) Reverse transcription-PCR analysis of pluripotency markers in both iPSC lines (iPSC-L1 and iPSC-L2, respectively). (**J**) Nanog expression (*green*) in iPSC-L2 iPSCs (DAPI = *blue*). (**I**, **L**) Teratoma formation assays for iPSC-L1 and iPSC-L2, respectively. ∧ = endoderm, * = ectoderm, + = mesoderm). *Scale bars*: 100 μm.

at the University of Iowa for karyotyping. Briefly, cells were arrested at metaphase with colcemid and the chromosomes stained by the G-banding method. The chromosomal number of each line was determined by microscopic analysis and the cells were examined for the presence or absence of detectable structural rearrangements. At least 5 cells from each line were analyzed and 3 cells from each line karyotyped. The karyotypes were prepared from computer-assisted digital images of the metaphases.

Statistical Analysis

To determine statistical significance, an unpaired *t*-test was performed using GraphPad Prism 6 software (GraphPad Software Co., La Jolla, CA, USA).

Results

Reprogramming Tie2-GFP Fibroblasts Into iPSCs

Tie2-GFP transgenic mice were used for these studies, because this mouse model expresses GFP under the control of the endothelial cell-specific angiopoietin receptor promoter, *Tie2*, resulting in GFP-positive endothelial cells (Fig. 1A).[12] To generate iPSCs, 1-week-old *Tie2-GFP* mice were euthanized, and dermal tail fibroblasts were harvested and cultured (Fig. 1B). Fibroblasts were expanded, passaged onto collagen-coated six-well culture plates at a density of 1×10^5 cells per well, and transduced with lentiviral constructs driving expression of the transcription factors *mKOrange2-Sox2*, *mEGFP-Oct4*, *mTagBFP-Klf4*, and *mKate-c-Myc* (fluorophore tags were included to confirm expression and reprograming). At 1 week following transduction, the cells were passaged onto IRR-MEFs and fed with pluripotency media. Approximately 10 days later, distinct colonies that expressed all four fluorophores were observed (Figs. 1C, 1D). These colonies displayed classic iPSC morphology with a large nuclei-to-cytoplasm ratio.[16,17]

Isolation and Characterization of Reprogrammed Tie2-GFP iPSCs

As the process of reprograming has been shown to induce expression of endogenous *Oct4, Sox2, Klf4 and c-Myc*, which in turn results in silencing of their transgenic counterparts, we decided to use the above-described flurophore tagged vectors to isolate and establish fully reprogrammed iPSC lines. To do so, iPSC colonies were passaged free from the underlying MEF feeder layer using collagenase and iPSCs no longer expressing fluorescent tags were sorted via FACS (Fig. 1D). The collected cells, hereafter referred to as iPSC Line 1 (iPSC-L1), were plated on IRR-MEFs and cells negative for fluorophore expression (Fig. 1E) were expanded clonally. To demonstrate pluripotency, immunocytochemistry, RT-PCR, and teratoma formation assays were performed. Immunocytochemical analysis demonstrated that undifferentiated iPSCs were positive for Nanog, a master regulator of pluripotency (Fig. 1F). Following embryoid body generation, *Tie2-GFP* positive cells were identified (Fig. 1G). Reverse transcription-PCR analysis demonstrated expression of the pluripotency markers *Dnmt1, Lin28, Nanog, Ssea-1*, and

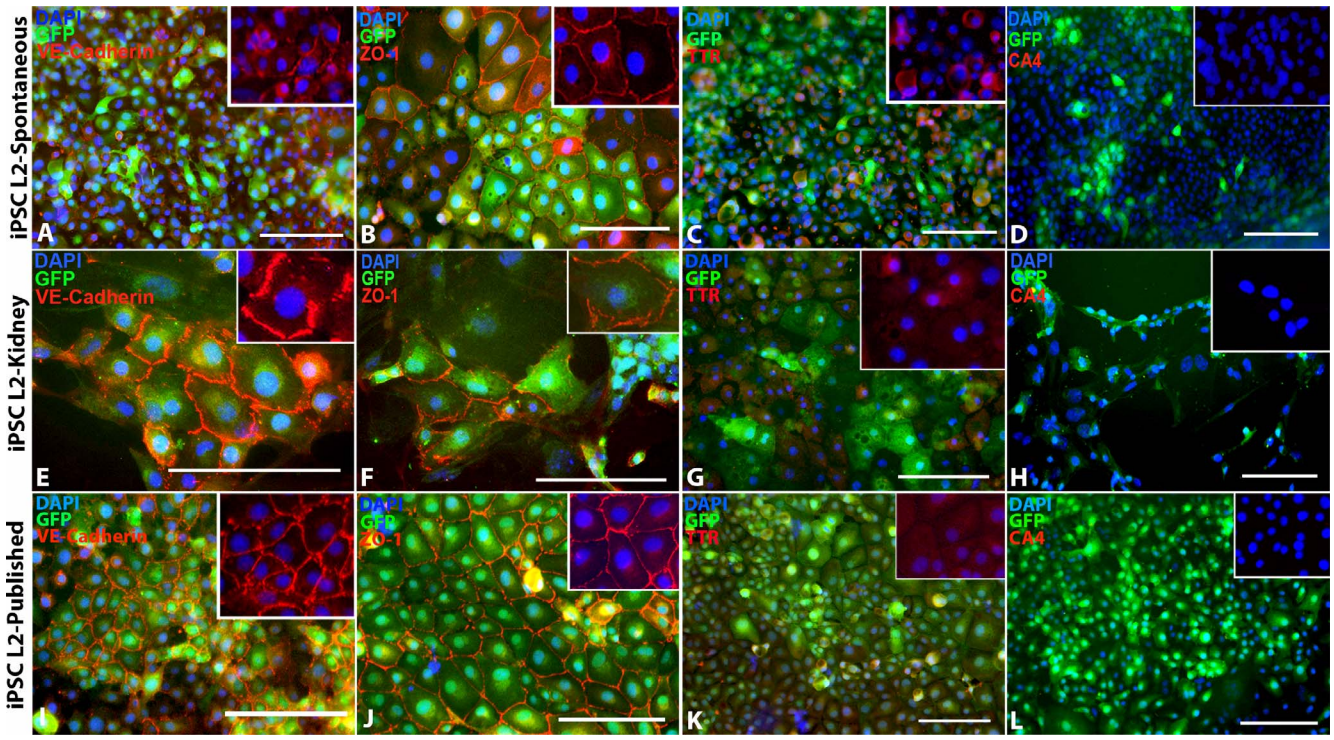

Figure 2. Spontaneous iPSC-EC differentiation, kidney coculture iPSC-EC differentiation, and previously published iPSC- EC differentiation protocol. (**A–D**) Spontaneously differentiated iPSC-derived ECs express EC markers (**A**) VE-Cadherin and (**B**) ZO-1, a small amount of (**C**) TTR, but no (**D**) CA4. (**E–H**) iPSC-derived ECs differentiated in coculture with primary mouse kidney ECs also express (**E**) VE-Cadherin, (**F**) ZO-1, and (**G**) TTR, but not (**H**) CA4. (**I–L**) Likewise, iPSC-derived ECs differentiated using a previously published iPSC-EC differentiation protocol from Rufaihah et al.[18] also express (**I**) VE-Cadherin, (**J**) ZO-1, and (**K**) TTR, but not (**L**) CA4. DAPI = *blue*. *Scale bars*: 100 μm.

Sox2 (Fig. 1H). At 8 weeks after intramuscular injection into immune compromised SCID mice, teratomas that contained cells of each of the three embryonic germ layers were detected (Fig. 1I). As indicated above, our goal was to use the *Tie2-GFP* reporter line to generate an iPSC choroidal endothelial cell generation protocol. As such, to corroborate our differentiation findings, a second iPSC line (iPSC-L2) was generated using a polycistronic lentiviral vector that lacked fluorescent reporters. In addition to having a second independently-generated iPSC line to validate differentiation protocols, this line also would alleviate concerns regarding specificity of GFP expression after differentiation (i.e., the only source of GFP in this line is under control of the Tie2 promoter). Like iPSC-L1, iPSC-L2 also expressed *Nanog* (Figs. 1J, 1K), *Dnmt1, Lin28, Ssea-1* and *Sox2*, (Fig. 1K), and formed teratomas in immunodeficient mice that contained tissues of each of the three embryonic germ layers (Fig. 1L).

Although iPSC-L1 and iPSC-L2 were determined to be pluripotent via this analysis, iPSC-L1 had a severely abnormal karyotype, that is, at multiple positions, multiple chromosomes were present (Supplementary Fig. S1). In light of this finding, the differentiation experiments presented below were performed using iPSC-L2 only.

Differentiation and Characterization of iPSC-Derived CECs

In an attempt to generate choroidal endothelial cells suitable for interrogation of disease pathophysiology and transplantation–based cell replacement, we began by testing the following three differentiation paradigms: (1) spontaneous differentiation (as per the methods section), (2) coculture of iPSCs with a peripheral vascular endothelial cell line (as per the methods section), and (3) a previously published vascular endothelial cell differentiation protocol.[18] Protocol efficacy was determined based on the ability to generate *Tie2-GFP*-positive cells expressing carbonic anhydrase IV (CA4), which in the retina is specific to the choriocapillaris (Supplementary Fig. S2).[19] As shown in Figure 2, by using the above 3 protocols, iPSC-derived endothelial cells positive for Tie2-GFP (Figs. 2A, 2E, 2I), ZO-1 (Figs. 2B, 2F, 2J), and TTR (Figs. 2C, 2G, 2K) were obtained. However, these cells were negative for the choroidal endothelial cell marker CA4 (Figs. 2D, 2H, 2L).

To determine if coculture with cells of choroidal origin could drive CA4 expression, EBs were cocultured with the monkey choroidal endothelial cell line, RF/6A (coculture differentiation strategy described in methods section and depicted in Fig. 3A). At 10 days after differentiation, as in the above differentiation experiment, a significant number of iPSC-derived GFP-positive cells were observed (Fig. 3B). Cultures subsequently were passaged and expanded for an additional 30 days. Immunostaining indicated that GFP-positive cells from each line expressed the choroid-specific marker carbonic anhydrase IV (CA4; Fig. 3C). Transthyretin (TTR, previously called prealbumin), is secreted from choroidal endothelial cells (Supplementary Fig. S2) and binds to retinol A.[20–22] To determine if iPSC-CECs expressed TTR, antibodies targeted against TTR were used. As shown in Figure 3, robust expression of TTR could be detected in GFP-positive iPSC-CECs (Figs. 3D, 3E). These cells also expressed FOXA2, an additional transcription factor expressed in choroidal endothelial cells (Fig. 3E).[23] In addition, the mature endothelial cell markers, VE-Cadherin (Figs. 3E, 3F) and ZO-1 (Fig. 3G) also were expressed. To determine if iPSC-derived pericytes were present in this culture system, an additional ICC experiment using antibodies targeted against α-SMA and NG2 proteoglycan

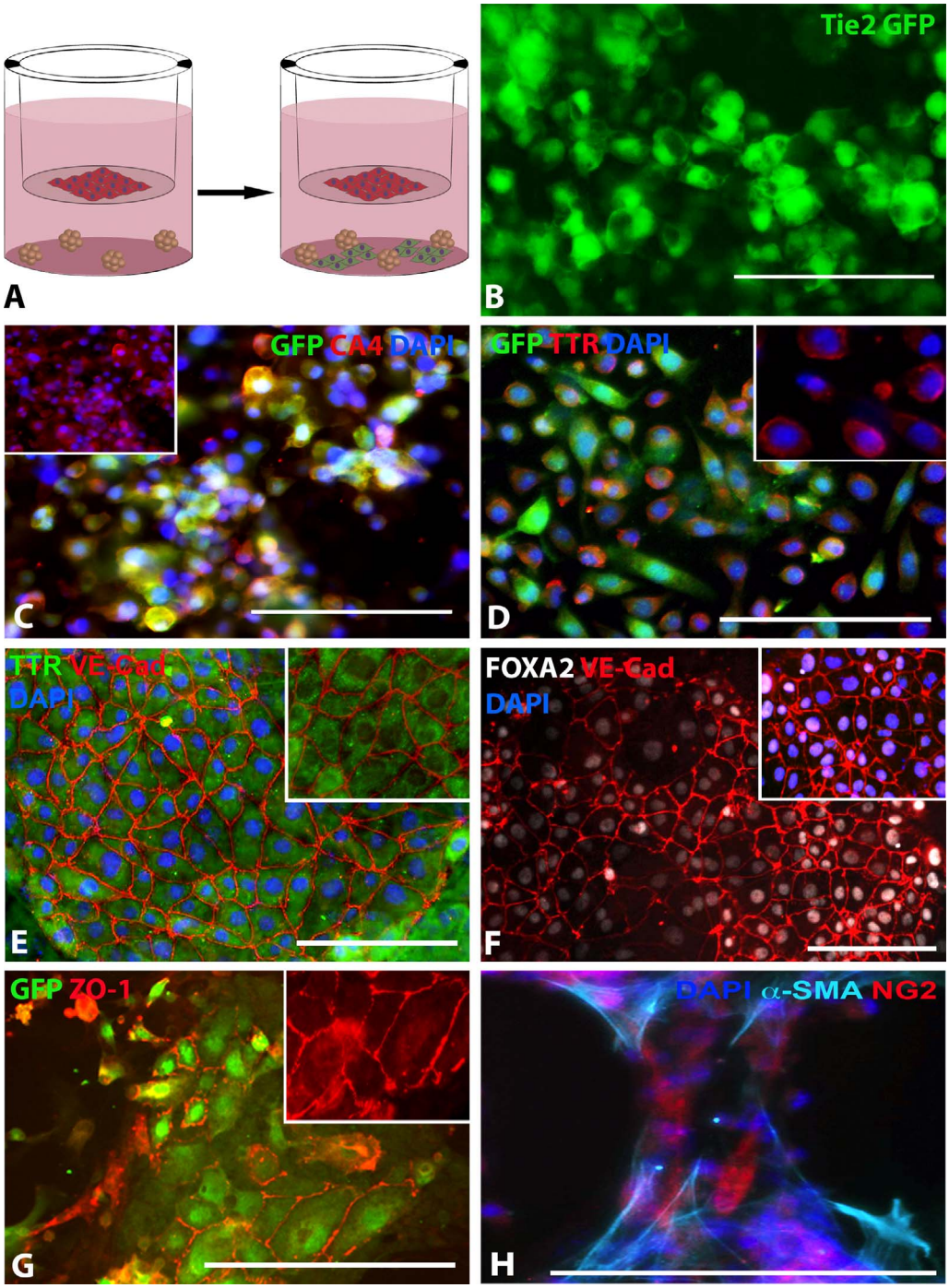

Figure 3. Differentiating choroidal-like ECs via co-culture with RF6A CECs. (**A**) Schematic illustrating differentiation paradigm: *red cells* = RF6A CECs, *green cells* = differentiated iPSC-ECs. (**B**) GFP expression in live iPSC-L2-RF6A ECs. (**C**) Carbonic anhydrase IV (CA4; *red*), GFP (*green*), and DAPI (*blue*) expression in iPSC-L2-RF/6A ECs; *inset* of only CA4 and DAPI expression. (**D**) GFP (*green*), TTR (*red*), and DAPI (*blue*) expression in iPSC-L2-RF/6A ECs, *inset* of only TTR and DAPI expression. (**E**) TTR (*green*), VE-Cadherin (*red*), and DAPI (*blue*) expression in iPSC-L2-RF/6A ECs; *inset* of only TTR and VE-Cadherin expression; pseudocoloring performed using Fiji. (**F**) Green fluorescent protein (*green*) and ZO-1 (*red*) expression in iPSC-L2-RF/6A ECs; *inset* of only ZO-1 expression. (**G**) FOXA2 (*gray*), VE-Cadherin (*red*), and DAPI (*blue*) expression in iPSC-L2-RF/6A ECs; pseudocoloring performed using Fiji. (**H**) α-SMA (*cyan*), NG-2 (*red*), and DAPI expression in iPSC-L2-RF/6A pericytes; pseudocoloring performed using Fiji. *Scale bars*: 100 μm.

was performed. As depicted in Figure 3, iPSC-derived cells positive for α-SMA and NG2 could be detected (Fig. 3H).[24]

To determine if the species of choroidal endothelial cells used to induce iPSC differentiation was important, that is, if mouse CECs induced enhanced differentiation when compared to monkey, primary CECs from 1-week-old mice were isolated (Figs. 4A, 4B) and cocultured with iPSC-L2 as described above. As demonstrated above, differentiated cells expressed GFP (Fig. 4C), CA4 (Fig. 4D), VE-Cadherin (Fig. 4E), and ZO-1 (Fig. 4F). Reverse transcription-PCR analysis showed that iPSC-CECs express the CEC-specific markers *CA4*, *FOXA2*, and *PLVAP* in addition to the pan EC markers *eNOS*, *CD31*,

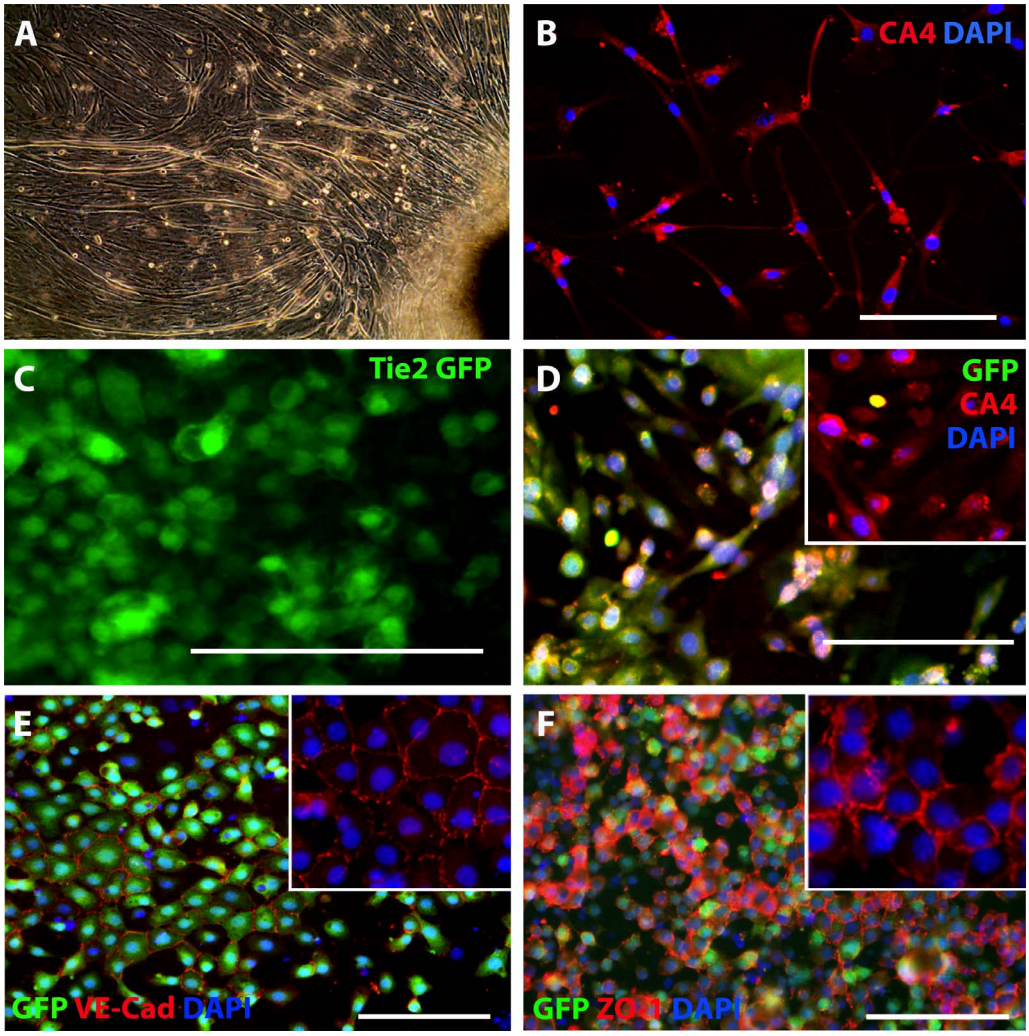

Figure 4. Differentiating choroidal-like ECs via coculture with primary CECs. (**A**, **F**) Isolated primary CECs from mouse choroids (CA4 = *red*, DAPI = *blue*). (**G–J**) iPSC-L2 differentiated in coculture with primary CECs. (**B**, **G**) Green fluorescent protein expression in live iPSC-L2-Prim ECs. (**C**, **H**) Carbonic anhydrase IV (CA4; *red*), GFP (*green*), and DAPI (*blue*) expression in iPSC-L2-Prim ECs; *insets* of CA4 and DAPI expression. (**D**, **I**) Green fluorescent protein (*green*), VE-Cadherin (*red*), and DAPI (*blue*) expression in iPSC-L2-Prim ECs. (**E**, **J**) Green fluorescent protein (*green*), ZO-1 (*red*), and DAPI (*blue*) expression in iPSC-L2-Prim ECs**.** *Scale bars*: 100 µm.

CD34, *Tie2*, *VE-Cadherin*, and *vWF* (Fig. 5A). When compared to other commercially available EC lines, the *Tie2-GFP* iPSC-derived CEC lines were most similar to primary CECs (Fig. 5A). In particular, aorta, brain and kidney vascular endothelial cells failed to express *CA4* while lung endothelial cells failed to express *FOXA2*, and aorta and lung cells fail to express *PLVAP* (Fig. 5A). To determine the efficiency of differentiation, iPSC-derived CEC cultures were analyzed using the Tali Image-Based Cytometer. Interestingly, the differentiation protocol, that is, the source of CECs used to induce differentiation, had no significant effect on the rate of CEC generation (Fig. 5B).

Discussion

Although the functions of the choroid are not completely understood, it is clear that this dense vascular bed is crucial for delivery of nutrients to the retina and for removal of waste products generated by photoreceptor and RPE cells. Damage to the choroid is detrimental and contributes to the pathophysiology of blinding retinal degenerative diseases by ischemia or other mechanisms. For instance, we have demonstrated previously that endothelial cells of the choriocapillaris are among the first to die in early AMD, when the RPE appears intact.[5–7,25] As photoreceptor, RPE, and choroidal endothelial cells are critically interdependent, that is, loss of one often results in death of the other, one could reason that early interventions focused on protection and/or replacement of choroidal endothelial cells before RPE and photoreceptor cell death could be a viable treatment option for AMD. Regardless of the sequelae of events in early AMD, however, patients with advanced AMD and extensive atrophy probably will require transplantation of choroidal endothelial cells, along with RPE and photoreceptor cells, to have their vision stably restored. For late stage disease, where extensive loss of all three cell types has occurred, transplant success likely will be dependent upon the use of supportive cell delivery systems designed to enhance cellular survival and integration after transplantation.[26–28] For instance, subretinal delivery of RPE cells in the form of single cell suspensions has been shown to result in poor donor cell survival[29,30]; this is true especially when transplanted onto atrophic Bruch's membranes.[31,32] To enhance RPE and photoreceptor cell survival, several groups have explored the use of various polymeric materials as cell delivery scaffolds. Diniz et al.[29] and Lu et al.[33] recently

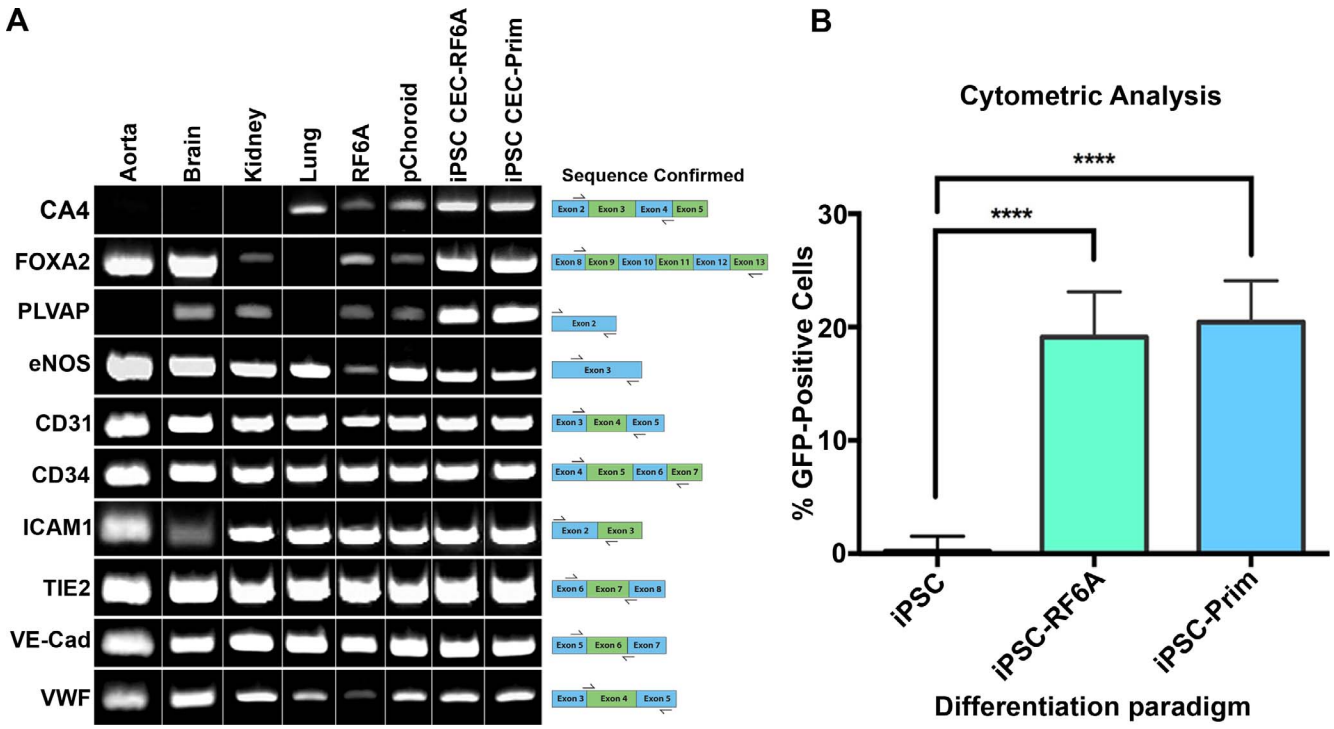

Figure 5. Comparing EC-specific marker expression in iPSC-ECs to other ECs and quantifying percentage of GFP-positive cells in iPSC-ECs. (**A**) Reverse transcription-PCR analysis of various EC markers in different cell types. (**B**) Tali cytometer analysis of iPSC-L2-RF6A and iPSC-L2-Prim lines compared to iPSC L2. $^{**}P \leq 0.01$; $^{***}P \leq 0.001$; $^{****}P \leq 0.0001$.

demonstrated that, compared to injection of single cells in suspension, RPE cell survival was significantly enhanced when delivered on parylene support membranes as polarized sheets. Importantly, while RPE sheet transplant allowed the investigators to deliver polarized RPE cell grafts at 1-month after injection, the majority of the donor RPE cells delivered in suspension were identified as clumped nonpolarized masses.[29] Photoreceptor cells have a similar need for support; we and others have shown that, compared to bolus cell injection, photoreceptor cell survival and integration is significantly enhanced when retinal progenitor cells are transplanted on polymer-based support systems.[27,28] Although the support structures developed in these studies were somewhat crude, new technologies, such as two-photon lithography, provide the level of resolution required to fabricate the highly organized structure of the outer retina.

To date, our group has successfully developed protocols to generate iPSC-derived photoreceptor and RPE cells from mice and humans.[16,17,34–36] In this study, we have demonstrated the successful generation of choroidal-like endothelial cells from an iPSC reporter line generated from the Tie2-GFP mouse, which is the first step in developing a step-wise iPSC-CEC differentiation protocol. The next step will be to determine the specific factors released by primary CECs that stimulate iPSC differentiation. Identifying said molecules would allow for the development of a clinically relevant xeno-free differentiation paradigm, which would ensure that immunogenic xeno antigens are not introduced. It is important to note that, although it is possible that the subretinal space is afforded some degree of immune privilege via the blood–retinal barrier (at least in a healthy eye), it is clear that the choriocapillaris is under full immune surveillance. As such, strategies focused on choroidal endothelial cell replacement would likely benefit from the use of autologous patient-specific iPSCs.

In addition to autologous transplantation, one of the great advantages of patient-specific iPSCs is their use in modeling different aspects of retinal degenerative diseases. Although significant advances have been made with respect to interrogation of mendelian disorders, using iPSCs to model complex diseases, such as AMD, which take decades to develop, is significantly more challenging. That said, by restricting the hypothesis one could envision a way in which iPSC-derived cells would be useful for interrogation of specific aspects of AMD. In particular, generation of patient-specific choroidal endothelial and RPE cells from patients with high risk and low risk CFH genotypes could be useful for determining which of these cell types are most impacted by complement insult.

Acknowledgments

The authors thank the Shivanand R. Patil Cytogenetics and Molecular Laboratory at the University of Iowa for performing the conventional cytogenetic analysis.

Supported in part by The Elmer and Sylvia Sramek Charitable Foundation, National Institutes of Health (NIH; Bethesda, MD, USA) Grants EY-024605 and 1-DP2-OD007483-01, Research to Prevent Blindness, and The Stephen A. Wynn Foundation. The University of Iowa Central Microscopy Research Facility is a core resource supported by the Vice President for Research & Economic Development, the Holden Comprehensive Cancer Center, and the Carver College of Medicine. The Flow Cytometry Facility at the University of Iowa is a Carver College of Medicine/Holden Comprehensive Cancer Center core research facility at the University of Iowa, supported by user fees and the Carver College of Medicine, Holden Comprehensive Cancer Center, and Iowa City Veteran's Administration Medical Center.

Disclosure: **A.E. Songstad**, None; **L.A. Wiley**, None; **K. Duong**, None; **E. Kaalberg**, None; **M.J. Flamme-Wiese**, None; **C.M. Cranston**, None; **M.J. Riker**, None; **D. Levasseur**, None; **E.M. Stone**, None; **R.F. Mullins**, None; **B.A. Tucker**, None

References

1. Buch H, Vinding T, La Cour M, Nielsen NV. The prevalence and causes of bilateral and unilateral blindness in an elderly urban Danish population. The Copenhagen City Eye Study. *Acta Ophthalmol Scand*. 2001;79:441–449.
2. Smith W, Assink J, Klein R, et al. Risk factors for age-related macular degeneration: pooled findings from three continents. *Ophthalmology*. 2001;108:697–704.
3. Friedman DS, O'Colmain BJ, Muñoz B, et al. Prevalence of age-related macular degeneration in the United States. *Arch Ophthalmol*. 2004;122:564–572.
4. VanNewkirk MR, Nanjan MB, Wang JJ, Mitchell P, Taylor HR, McCarty CA. The prevalence of age-related maculopathy: the visual impairment project. *Ophthalmology*. 2000;107:1593–1600.
5. Whitmore SS, Braun TA, Skeie JM, et al. Altered gene expression in dry age-related macular degeneration suggests early loss of choroidal endothelial cells. *Mol Vis*. 2013;19:2274–2297.
6. Mullins RF, Johnson MN, Faidley EA, Skeie JM, Huang J. Choriocapillaris vascular dropout related to density of drusen in human eyes with early age-related macular degeneration. *Invest Ophthalmol Vis Sci*. 2011;52:1606–1612.
7. Sohn EH, Khanna A, Tucker BA, Abramoff MD, Stone EM, Mullins RF. Structural and biochemical analyses of choroidal thickness in human donor eyes. *Invest Ophthalmol Vis Sci*. 2014;55:1352–1360.
8. Almeida DRP, Zhang L, Chin EK, et al. Comparison of retinal and choriocapillaris thicknesses following sitting to supine transition in healthy individuals and patients with age-related macular degeneration. *JAMA Ophthalmol*. 2015;133:297–303.
9. Mullins RF, Schoo DP, Sohn EH, et al. The membrane attack complex in aging human choriocapillaris: relationship to macular degeneration and choroidal thinning. *Am J Pathol*. 2014;184:3142–3153.
10. Age-Related Eye Disease Study Research Group. A randomized, placebo-controlled, clinical trial of high-dose supplementation with vitamins C and E, beta carotene, and zinc for age-related macular degeneration and vision loss: AREDS report no. 8. *Arch Ophthalmol*. 2001;119:1417–1436.
11. Hogan MJ. Role of the retinal pigment epithelium in macular disease. *Trans Am Acad Ophthalmol Otolaryngol*. 1972;76:64–80.
12. Motoike T, Loughna S, Perens E, et al. Universal GFP reporter for the study of vascular development. *Genesis*. 2000;28:75–81.
13. Levasseur DN, Ryan TM, Pawlik KM, Townes TM. Correction of a mouse model of sickle cell disease: lentiviral/antisickling beta-globin gene transduction of unmobilized, purified hematopoietic stem cells. *Blood*. 2003;102:4312–4319.
14. Duong KL, Das S, Yu S, et al. Identification of hematopoietic-specific regulatory elements from the CD45 gene and use for lentiviral tracking of transplanted cells. *Exp Hematol*. 2014;42:761–72.e1.
15. Schindelin J, Arganda-Carreras I, Frise E, et al. Fiji: an open-source platform for biological-image analysis. *Nat Methods*. 2012;9:676–682.
16. Tucker BA, Scheetz TE, Mullins RF, et al. Exome sequencing and analysis of induced pluripotent stem cells identify the cilia-related gene male germ cell-associated kinase (MAK) as a cause of retinitis pigmentosa. *Proc Natl Acad Sci USA*. 2011;108:E569–E576.
17. Tucker BA, Mullins RF, Streb LM, et al. Patient-specific iPSC-derived photoreceptor precursor cells as a means to investigate retinitis pigmentosa. *Elife*. 2013;2:e00824.
18. Rufaihah AJ, Huang NF, Kim J, et al. Human induced pluripotent stem cell-derived endothelial cells exhibit functional heterogeneity. *Am J Transl Res*. 2013;5:21–35.
19. Baba T, Grebe R, Hasegawa T, et al. Maturation of the fetal human choriocapillaris. *Invest Ophthalmol Vis Sci*. 2009;50:3503–3511.
20. Pino RM. Restriction of exogenous transthyretin (prealbumin) by the endothelium of the rat choriocapillaris. *Am J Anat*. 1986;177:63–70.
21. Dwork AJ, Cavallaro T, Martone RL, Goodman DS, Schon EA, Herbert J. Distribution of transthyretin in the rat eye. *Invest Ophthalmol Vis Sci*. 1990;31:489–496.
22. Smith SS, Pino RM, Thouron CL. Binding and transport of transthyretin-gold by the endothelium of the rat choriocapillaris. *J Histochem Cytochem*. 1989;37:1497–1502.
23. Tosi J, Janisch KM, Wang N-K, et al. Cellular and molecular origin of circumpapillary dysgenesis of the pigment epithelium. *Ophthalmology*. 2009;116:971–980.
24. Lutty GA, Hasegawa T, Baba T, Grebe R, Bhutto I, McLeod DS. Development of the human choriocapillaris. *Eye (Lond)*. 2010;24:408–415.
25. Coscas F, Puche N, Coscas G, et al. Comparison of macular choroidal thickness in adult onset foveomacular vitelliform dystrophy and age-related macular degeneration. *Invest Ophthalmol Vis Sci*. 2014;55:64–69.
26. Yao J, Ko CW, Baranov PY, et al. Enhanced differentiation and delivery of mouse retinal progenitor cells using a micropatterned biodegradable thin-film polycaprolactone scaffold. *Tissue Eng Part A*. 2015;21:1247–1260.
27. Tucker BA, Redenti SM, Jiang C, et al. The use of progenitor cell/biodegradable MMP2-PLGA polymer constructs to enhance cellular integration and retinal repopulation. *Biomaterials*. 2010;31:9–19.
28. Tomita M, Lavik E, Klassen H, Zahir T, Langer R, Young MJ. Biodegradable polymer composite grafts promote the survival and differentiation of retinal progenitor cells. *Stem Cells*. 2005;23:1579–1588.
29. Diniz B, Thomas P, Thomas B, et al. Subretinal implantation of retinal pigment epithelial cells derived from human embryonic stem cells: improved survival when implanted as a monolayer. *Invest Ophthalmol Vis Sci*. 2013;54:5087–5096.
30. Hu Y, Liu L, Lu B, et al. A novel approach for subretinal implantation of ultrathin substrates containing stem cell-derived retinal pigment epithelium monolayer. *Ophthalmic Res*. 2012;48:186–191.
31. Gullapalli VK, Sugino IK, Van Patten Y, Shah S, Zarbin MA. Retinal pigment epithelium resurfacing of aged submacular human Bruch's membrane. *Trans Am Ophthalmol Soc*. 2004;102:123–137.
32. Gullapalli VK, Sugino IK, Van Patten Y, Shah S, Zarbin MA. Impaired RPE survival on aged submacular human Bruch's membrane. *Exp Eye Res*. 2005;80:235–248.
33. Lu B, Zhu D, Hinton D, Humayun MS, Tai Y-C Mesh-supported submicron parylene-C membranes for culturing retinal pigment epithelial cells. *Biomed Microdevices*. 2012;14:659–667.
34. Tucker BA, Anfinson KR, Mullins RF, Stone EM, Young MJ. Use of a synthetic xeno-free culture substrate for induced pluripotent stem cell induction and retinal differentiation. *Stem Cells Transl Med*. 2013;2:16–24.
35. Tucker BA, Solivan-Timpe F, Roos BR, et al. Duplication of TBK1 stimulates autophagy in iPSC-derived retinal cells from a patient with normal tension glaucoma. *J Stem Cell Res Ther*. 2014;3:161.
36. Tucker BA, Park I-H, Qi SD, et al. Transplantation of adult mouse iPS cell-derived photoreceptor precursors restores retinal structure and function in degenerative mice. *PLoS One*. 2011;6:e18992.